**Northwest Africa 2975** – 70.1 grams

**NWA2986** – 201 grams **NWA2987** – 225 grams ?

**NWA4766** – 47 grams **NWA4783** – 120 grams

**NWA4857** – 24 grams **NWA4864** – 94 grams

**NWA4878** – 130 grams **NWA4880** – 81.6 grams

**NWA4930** – 117.5 grams **NWA5140** – 7.5 grams

**NWA5214** – 50.7 grams **NWA5219** – 60 grams

**NWA5313** – 5.3 grams **NWA5366** – 39.6 grams

Enriched fine-grained shergottite

(shower) ~1.6 kg

***Figure 1:*** *Photograph of NWA 2975 taken by Mike Farmer. Cube is 1 cm.*

**Introduction**

Abstracts by Wittke *et al.* (2006) and Bunch *et al.* (2008) describe a shower of small (~100 g each) bits and pieces of basaltitc shergottite (*there may be over a hundred pieces*). Many have a fresh fusion crust (partial), a basaltic texture and the characteristic glass pockets and thin black glass veins such as are seen in Zagami and other basaltic shergottites. These glass pockets will prove important (*see sections on EETA79001 and Zagami*).

The first specimen, NWA 2975, was originally purchased by Mike Farmer in Erfoud, Morocco, but the suspected strewnfield is thought to be in Algeria (Bunch et al., 2008). Since then additional members have been found, including NWA 2986, 2987, 4766, 4783, 4857, 4864, 4878, 4880, 4930, 5140, 5214, 5219, 5313, and 5366 (Figures 2 to 6).

***Figure 2:*** *Interior of NWA 2975 showing vesicular glass pockets and veins. Photo by Mike Farmer.*

**Petrography**

According to Wittke *et al.* (2006), NWA 2975 is a fresh, medium-grained, subophitic to granular hypabyssal basalt with intergrown prismatic pyroxene and plagioclase grains up to 3 mm long (Figure 7). The hand specimen also exhibits vesicular black glass veins up to 3 mm wide and glass pockets up to 6 mm (Figure 2). Accessory phases include ülvospinel, ilmenite (Figure 8), chlorapatite, merrillite, pyrrhotite, Si-Al-K-Na-rich glass and baddeleyite. Large ülvospinel grains contain melt inclusions.

***Figure 3:*** *Sawn surface of NWA 4766 (photo by S. Ralew).*

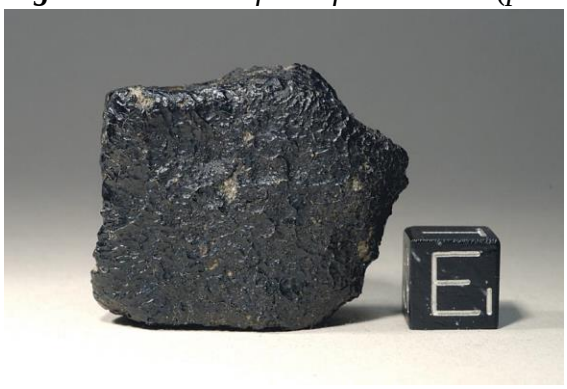

***Figure 4a,b:*** *Fusion crust on outer surface and sawn surface of NWA 4766 (photos by S. Ralew).*

***Figure 5 (left):*** *Photo of ablation surface of NWA 4880 (photo from "Hupe Collection").*
***Figure 6 (right):*** *Exterior of NWA 2986 (photo by J. Farmer).*

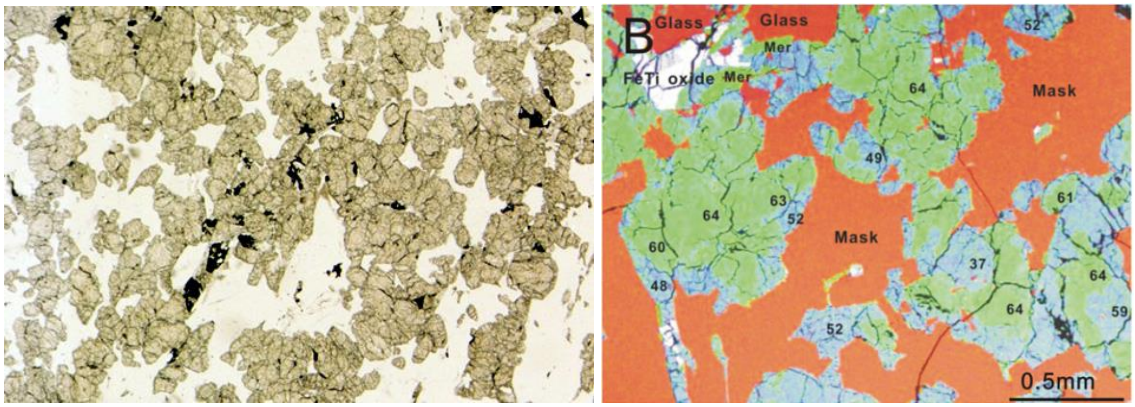


***Figure 7a:*** *Photomicrograph of thin section of NWA 2986 (J. Wittke and T. Bunch). Photo is 8 mm across.* ***Figure 7b:*** *False color image of combined X-ray Ca (green)-Fe (blue)-Al (red). The numbers shown are the Mg# number of the pyroxenes (from He et al., 2015).*

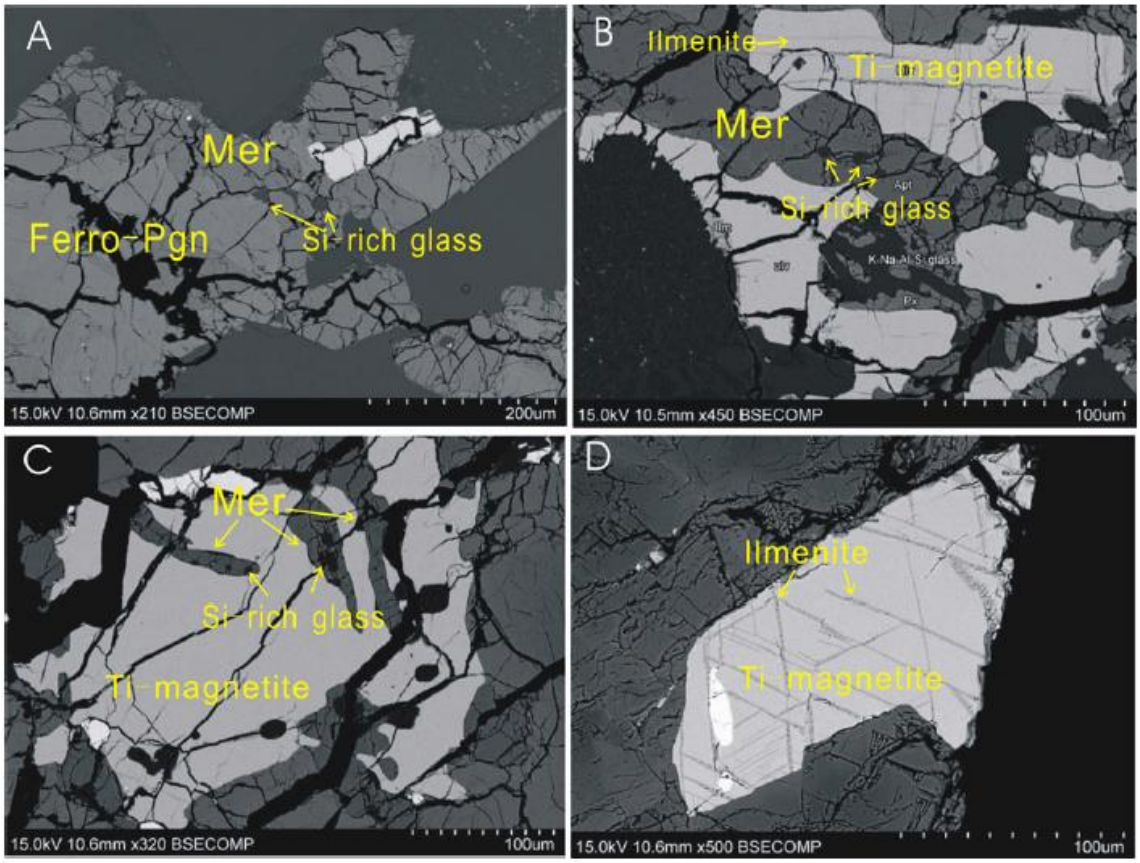


***Figure 8:*** *Petrographic features of phosphates and Fe-Ti oxides in NWA 2975. A) phosphate (Mer) and Si-rich melts intruded in grains Fe-rich pigeonite (Ferro-Pgn). B and C) Trapped melt inclusions or phosphate and Si-rich melts intruded in grains of Fe-Ti oxides. The melts exhibit marginal rims of Fe-rich pigeonite + merrillite surrounding cores of Si-Al-K-Na-rich glass in image (B). D) Ti-magnetite grains have ilmenite exsolution lamellae. Images and figure from He et al., 2015.*

**Mineralogical Mode for NWA2975**

| | **Wittke et al. 2006** |
|---|---|
| Pyroxene | 57.3 vol. % |
| Plagioclase | 38.3 (maskelynite) |
| Opaques | 2.7 |
| Phosphate | 1.7 |

**Mineral Chemistry**

***Pyroxenes***: The pyroxenes in NWA 2975 are relatively iron rich with exsolution features (Figure 9). Both augite and pigeonite are present. The Mn/Fe ratio demonstrates samples are Martian.

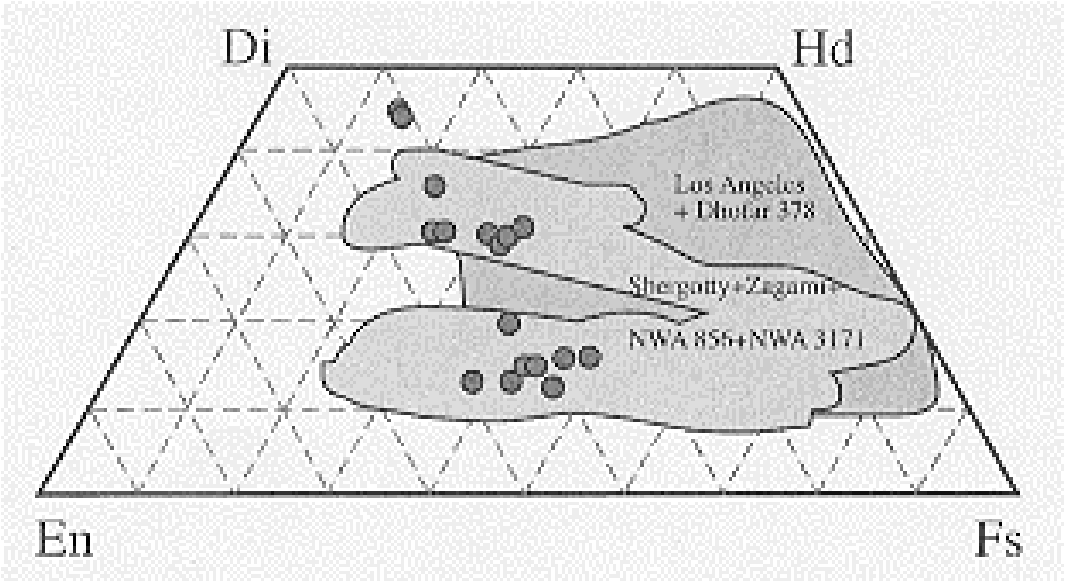


***Figure 9:*** *Pyroxene composition of NWA 2975 compared with that of some other martian shergottites (from Wittke et al., 2006).*

***Maskelynite***: Plagioclase in NWA2975 has entirely been converted to maskelynite $An_{55}$ (Wittke et al. 2006).

***Glass:*** Glass pockets are vesicular.

***Chromite:*** Ülvospinel.

***Sulfide:*** Pyrrhotite.

***Phosphate:*** NWA 2975 and NWA 4864 have reported merrillite and apatite (Channon et al. 2011; Slaby et al., 2016, 2017; Shearer et al., 2015). The apatite studied by Slaby et al. (2016) is F-rich hydroxyl-apatite (Figure 10). Slaby et al. (2017) found a more diverse phosphate assemblage and proposed the crystallization of two generations of fluorapatite: apatite crystals crystallized from an evolved, differentiated, and degassed magma, whereas chlorapatite replaced ferromerrillite-merrillite and was not related to the mantle-derived shergottite magma. The relationship between merrillite and apatite indicates that

apatite is most probably a product of merrillite reacting with fluids. (Figure 11). Slaby et al. (2017) suggest that only the fluorapatite (F > Cl~OH) is a reliable source for assessing the degree of Martian mantle hydration. In addition, Ward et al. (2017) report REE and other trace element data for the apatite and merrillite from NWA 4864, showing its similarity to other shergottite merrillites (Figures 12 and 13)

***Ilmenite:*** Attached to ülvospinel.

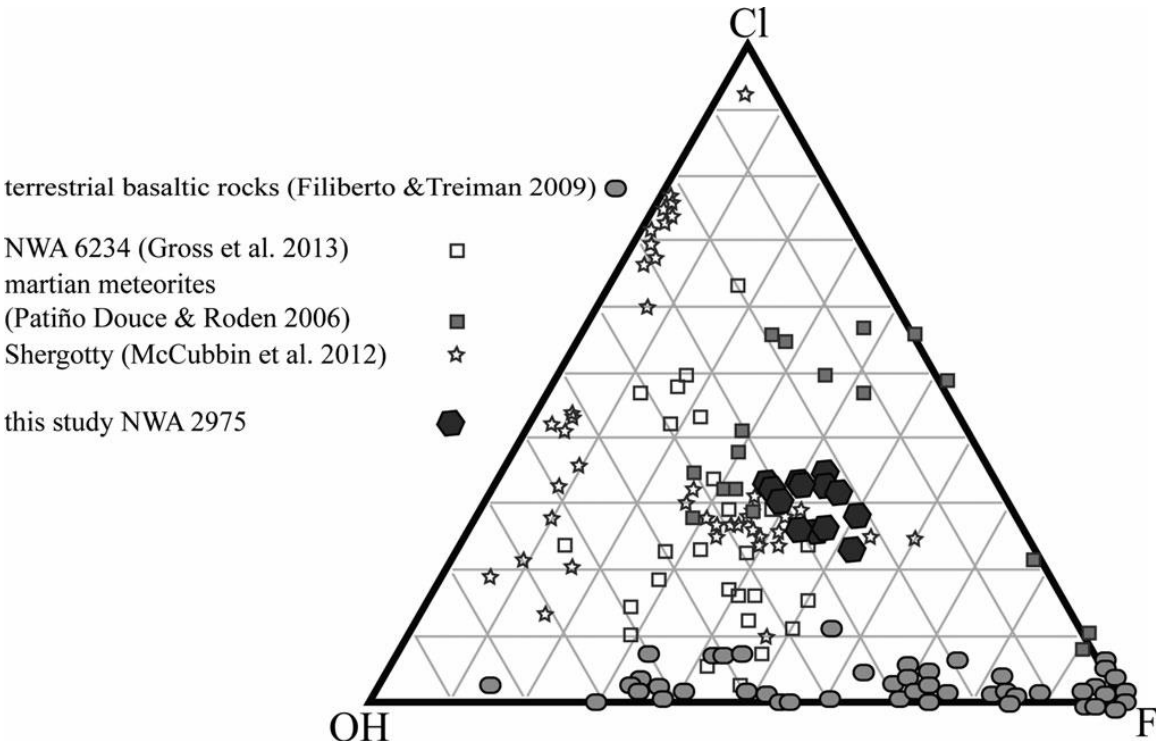


***Figure 10:*** *Cl-OH-F ternary diagram for apatite from NWA 2975 (from Slaby et al., 2016).*

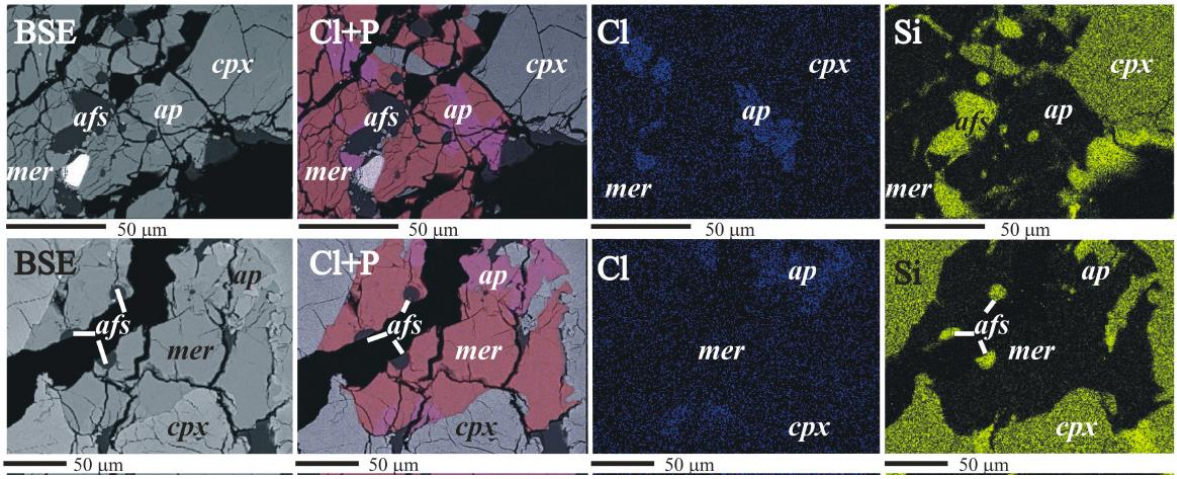


***Figure 11:*** *Two examples of the textural relations between apatite and merrillite in NWA 2975 (from Slaby et al., 2017).*

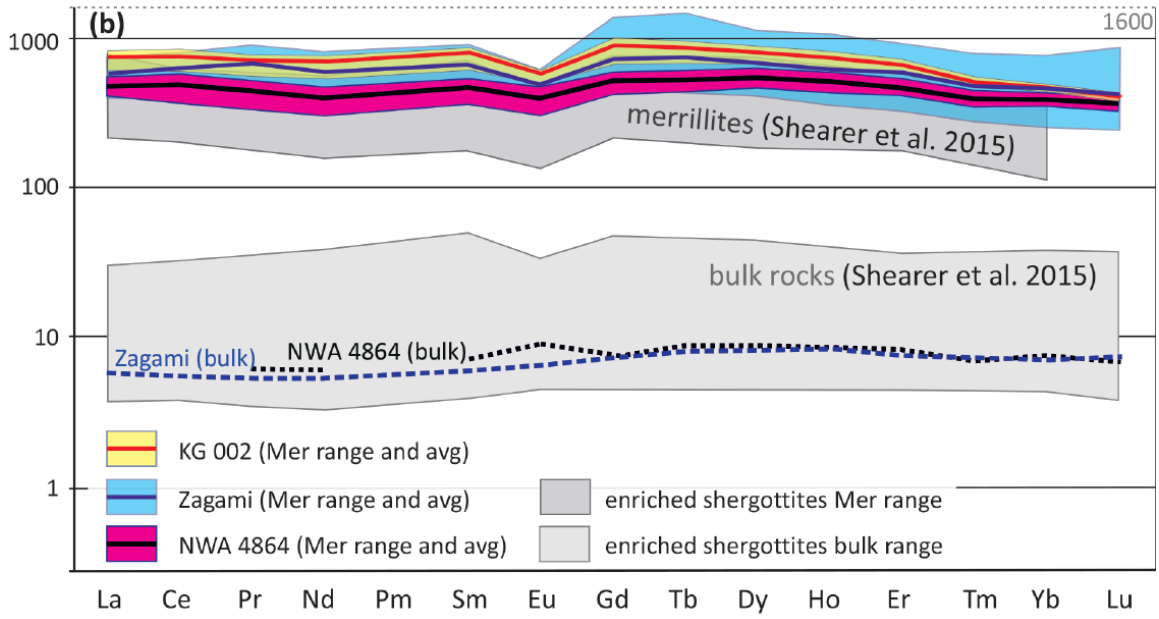


***Figure 12:*** *REE patterns for merrillite from NWA 4864 showing its similarity to other shergottite merrillites (from Ward et al., 2017).*

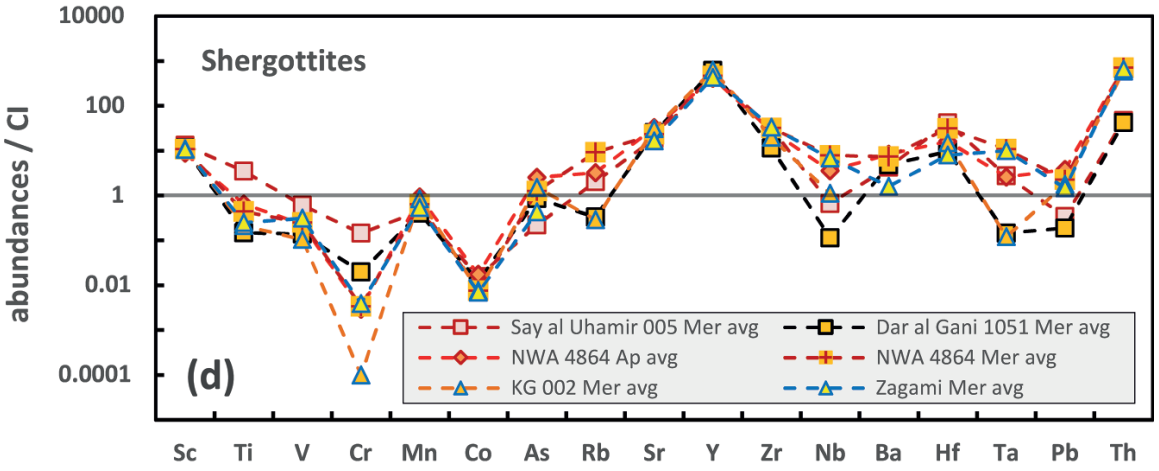


***Figure 13:*** *Trace element patterns for apatite and merrillite from NWA 4864 showing their similarity to each other and to those in other shergottites (from Ward et al., 2017).*

**Table 1. Chemical composition of NWA 2975 and pairs.**

| *reference* | Weisberg (2986) | Yang (5214) |
|---|---|---|
| *weight* | | |
| *technique* | *ICP-MS* | *LA-ICP-MS* |
| | | |
| $SiO_2$ % | | 47.4 |
| $TiO_2$ | | 0.87 |
| $Al_2O_3$ | | 6.50 |

| | | |
|---|---|---|
| FeO | | 20.54 |
| MnO | | 0.563 |
| MgO | | 8.42 |
| CaO | | 12.39 |
| $Na_2O$ | | 1.5 |
| $K_2O$ | | 0.34 |
| $P_2O_5$ | | 1.45 |
| S % | | 0.03 |
| *sum* | | |
| | | |
| Sc ppm | | 73 |
| V | 236 | 320 |
| Cr | 646 | 832 |
| Co | 29 | 37 |
| Ni | 47 | 51 |
| Cu | | 13.8 |
| Zn | | 81 |
| Ga | | 17.0 |
| Ge | | 1.36 |
| As ppb | | 350 |
| Se | | 400 |
| Rb ppm | | 17.7 |
| Sr | | 63 |
| Y | | 29 |
| Zr | | 74 |
| Nb | | 4.06 |
| Mo | | - |
| Ru ppb | | - |
| Rh | | - |
| Pd | | - |
| Ag | | 7 |
| Cd | | - |
| In | | 69 |
| Sn | | 404 |
| Sb | | 14 |
| Te | | - |
| Cs | | 1135 |
| Ba ppm | 21 | 45.7 |
| La | 0.97 | 3.93 |
| Ce | 2.32 | 9.50 |
| Pr | | 1.38 |
| Nd | 1.7 | 6.98 |
| Sm | 0.71 | 2.67 |
| Eu | 0.43 | 0.95 |
| Gd | 1.71 | 4.40 |
| Tb | | 0.81 |
| Dy | 1.12 | 5.42 |
| Ho | | 1.12 |
| Er | | 3.13 |
| Tm | | 0.43 |
| Yb | 0.85 | 2.67 |
| Lu | 0.12 | 0.38 |
| Hf | 1.07 | 2.23 |
| Ta ppb | | 187 |
| W ppb | | 451 |

| | |
|---|---|
| Re ppb | - |
| Os ppb | 0.86 |
| Ir ppb | 0.18 |
| Pt ppb | 0.7 |
| Au ppb | 0.6 |
| Tl | 38 |
| Pb ppm | 1.15 |
| Bi ppb | 29.0 |
| Th ppb | 602 |
| U ppb | 154 |

## Whole-rock Composition

Weisberg *et al.* (2010) reported a preliminary analysis of NWA 2986 (Table 1). NWA 5214 was analyzed for a more extensive list of elements which clearly show the evolved and enriched nature of this basaltic shergottite (Yang et al., 2015). The siderophile elements were used to help constrain the conditions of core-mantle differentiation in Mars, and the Ge contents have been used to understand magmatic degassing processes (Humayun et al., 2016; Yang et al. 2018).

Sanborn and Wadhwa (2010) were able to determine that the minerals in NWA 2975 crystallized from an "enriched" magma. Wittke *et al.* (2010) reported a difference in composition of NWA 5718 and NWA 2975, indicating that NWA 5718 is not paired. The REE contents of the individual phases in NWA 2975 are nearly identical to those in Shergotty and Zagami (Figure 14), demonstrating the overall similarity in composition between all these enriched shergottites.

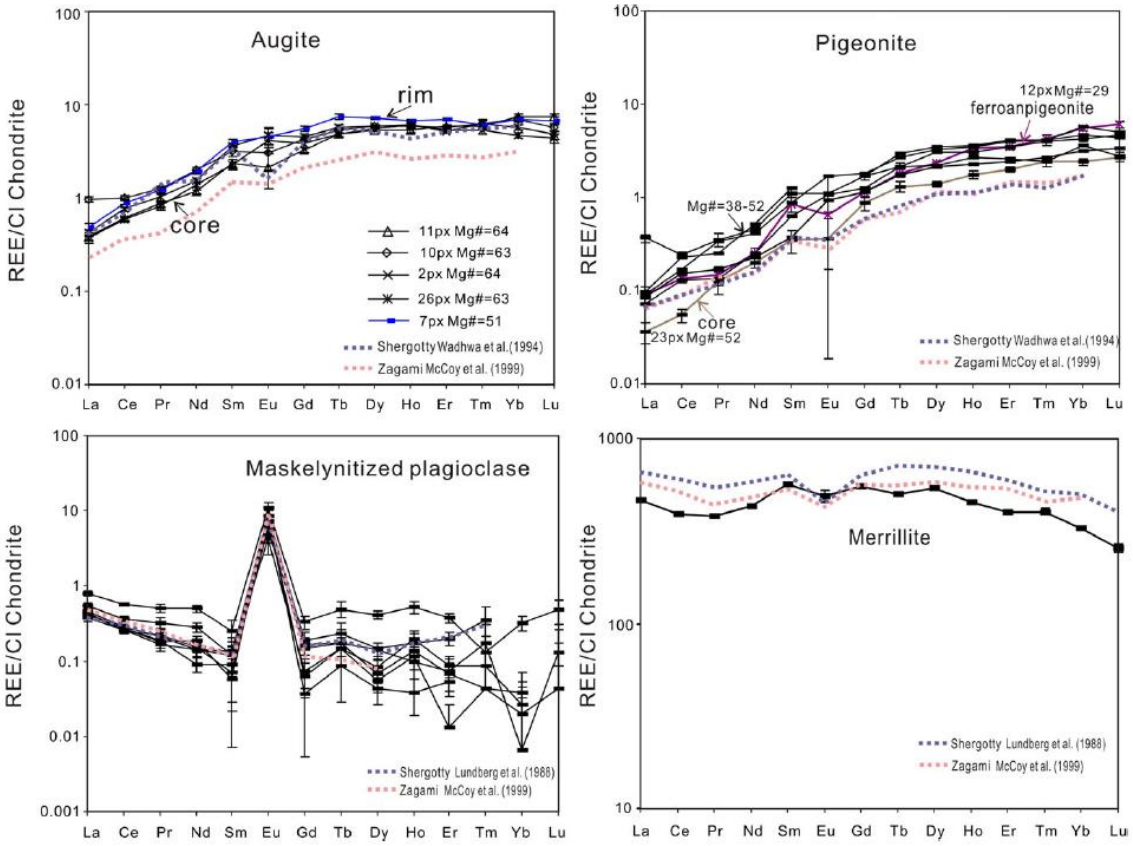


***Figure 14:*** *Representative REE concentrations of pyroxenes, maskelynite, and merrillite of NWA 2975. For comparison, the mineral compositions of Shergotty and Zagami are shown after Wadhwa et al. (1994) and McCoy et al. (1999).*

## Radiogenic Isotopes

Cassata and Borg (2016) report Ar-Ar data for NWA 2975 and calculate an age of 184 +/- 17 Ma when corrected for the trapped $^{36}$Ar component (Figure 15). This is in reasonable agreement with Borg et al. (2016) who measured Rb-Sr and Sm-Nd isotopes in NWA 4878 and demonstrate its young age (170 Ma; Borg et al., 2016), similar to other enriched basaltic shergottites. In addition, they demonstrated, together with analyses of many other martian meteorites, that the age of the sources region must be ~ 4.5 Ga (Figure 16).

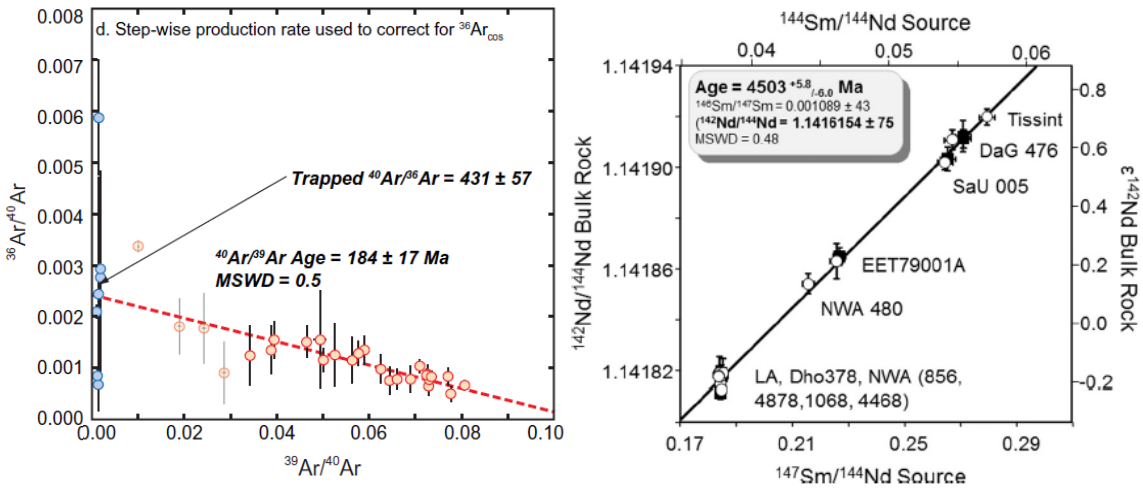


***Figure 15:*** *$^{36}Ar/^{40}Ar$ versus $^{39}Ar/^{40}Ar$ plot for NWA 2975 showing the result of corrections due to $^{36}Ar$ cosmogenic, which lead to an age of 184 +/- 17 Ma (from Cassata and Borg, 2016).*

***Figure 16:*** *A $^{146}Sm$-$^{142}Nd$ isochron plot used to determine the age of formation of the shergottite source regions. This isochron yields a $^{146}Sm/^{147}Sm$ slope of 0.001089 ± 43 (MSWD = 0.48) that corresponds to an age of 4503 ± 6 Ma. Diagram from Borg et al. (2016).*

## Cosmogenic Isotopes

Berezhnoy *et al.* (2008) determined that $^{10}Be$, $^{26}Al$ and $^{53}Mn$ activity of NWA 2975. They calculate a cosmic ray exposure age of 1.6 m.y. Cassata and Borg (2016) determined cosmic ray exposure age from Ar analyses of un-irradiated aliquots of maskelynite and obtained an age of 1.62 +/- 0.10 Ma.

## Other Isotopes

Many stable isotope studies are aimed at deciphering the building blocks of Mars, such as Li, Mg, and Cl isotopes:

*Li* - Lithium isotopes have been measured for NWA 4864, and have helped to define the Li isotopic composition of the martian mantle (Magna et al., 2015), which has facilitated studies of the role of mantle versus crustal assimilation in generating shergottites (Figure 17), and also comparative planet accretion by comparison to the martian values to Earth, Moon and asteroid 4 Vesta. This work by Magna estimated the $\delta^7Li$ for Mars to be 4.2 +/- 0.9, within error of the estimate for Earth's mantle 3.5 +/- 1.0 (Magna et al., 2015).

*Mg* - Magna et al. (2017) examined Mg isotopic composition of a suite of Martian meteorites and made a similar finding to that for Li and Ca – that Mars silicate mantle has a $\delta^{26}Mg$ value that is identical to that for the rest of the inner solar system.

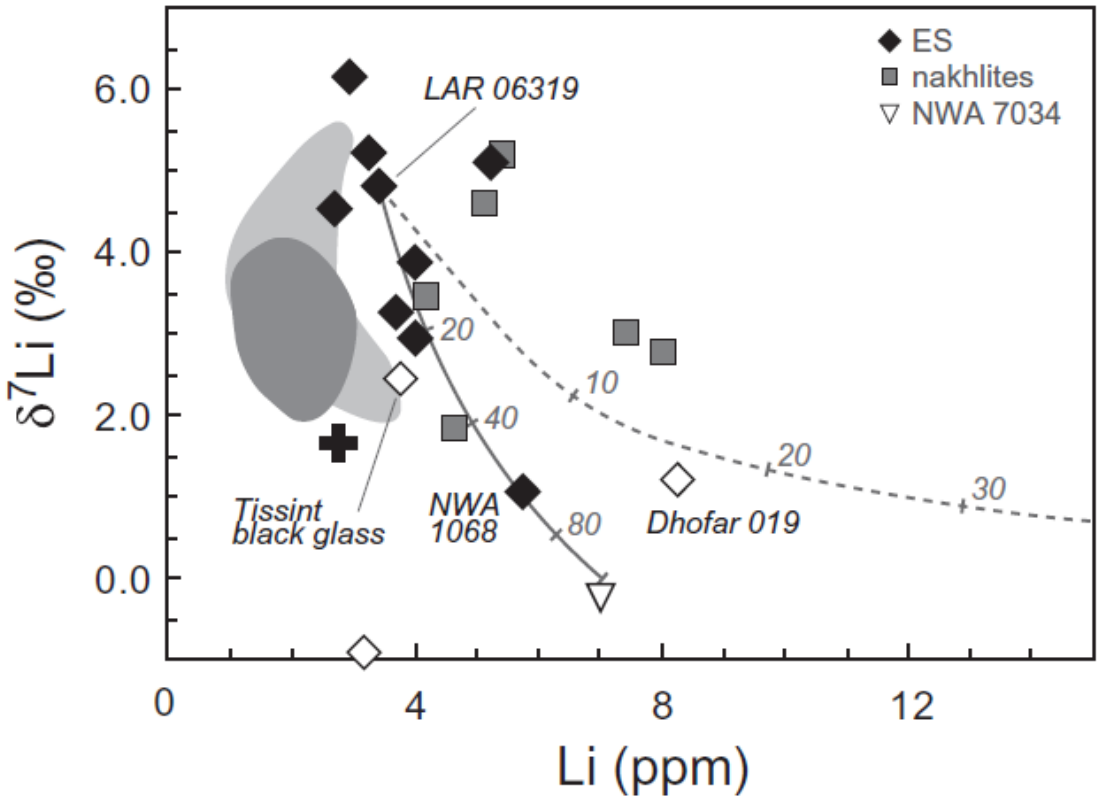


***Figure 17:*** *Simple binary mixing model between the estimated mantle source composition of enriched shergottites, closely resembling that of Shergotty and LAR 06319, and NWA 7034. A dashed mixing line constructed with the terrestrial upper continental crust composition (from Teng et al., 2004) illustrates that an analogous type of evolved crust on Mars cannot account for Li contents and isotope compositions recorded in most shergottites. Dark gray field – intermediate shergottites; medium gray field – depleted shergottites. Diagram from Magna et al. (2015). NWA 4864 plots at 4 ppm Li and 2.95* $\delta^7$*Li (per mil).*

Cl - Williams et al. (2016) and Sharp et al. (2016) measured Cl isotopes in Martian meteorites and proposed that the lightest values of $\delta^{37}$Cl (~ -4) represent the mantle and that heavier values up to ~ +1, represent interaction with crust or surface lithologies (Figure 18). This interpretation is at odds with that of Bellucci et al. (2017) who measured Cl isotopes and halogens in phosphates from Martian meteorites. They conclude that phosphates with no textural, major element, or halogen enrichment evidence for mixing with this surface reservoir have an average $\delta^{37}$Cl of −0.6‰, which supports a similar initial Cl isotope composition for Mars, the Earth, and the Moon. Oxidation and reduction of chlorine are the only processes known to strongly fractionate Cl isotopes (both (+)ve and (-)ve), and perchlorate has been detected on the Martian surface, which has 5000 ppm Cl (Figure 20). Perchlorate formation and halogen cycling

via brines has been active throughout Martian history, and has a significant influence of the Cl isotopic composition (Figure 19).

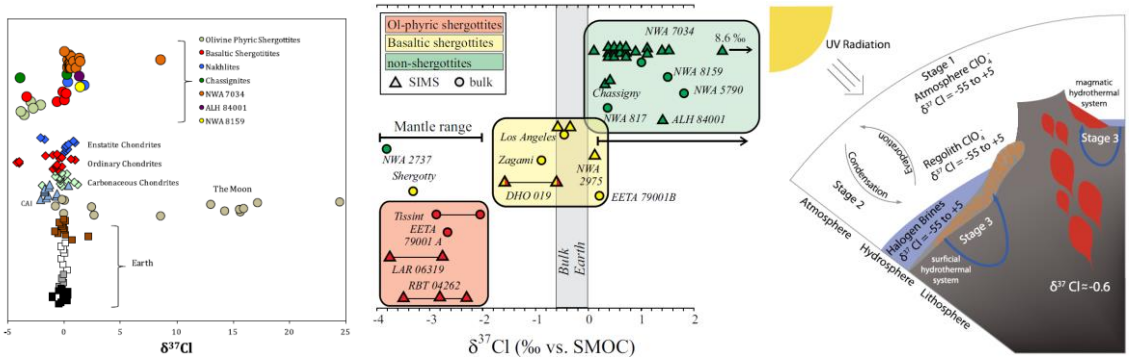


***Figure 18:*** *Chlorine isotopic composition of Martian meteorites determined by Williams et al. (2016) (left) and Sharp et al. (2016) (center). The lightest values among the Martian meteorites are interpreted as representative of the mantle.*

***Figure 19 (right):*** *Schematic illustration of the possible source of Martian light and heavy chlorine isotopic values measured in Martian meteorites (from Bellucci et al., 2017).*

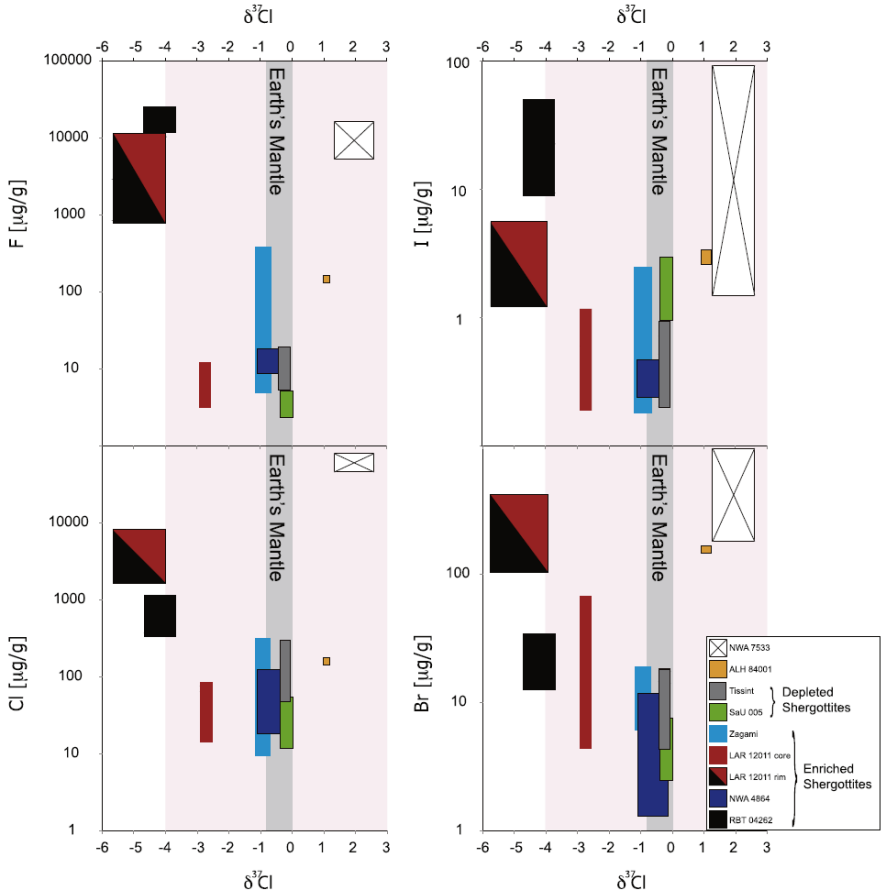


***Figure 20:*** *from Bellucci et al. (2017) showing variation of halogens with Cl isotopic composition.*

Measurements of the short-lived isotopic systems Hf-W and Sm-Nd can be used to place constraints on the timing of differentiation in Mars. Measurements of NWA 4864 yield $\varepsilon^{182}W$= 0.35 ±0.10 $\varepsilon^{142}Nd$ = -0.19 ±0.06 (Kruijer et al., 2017; Figure 21). These values, when combined with results of depleted and more enriched Martian meteorites, show that the Martian mantle differentiated between 25 and 35 Ma after $T_0$.

NWA 4864 samples were part of a study of Ba isotopes in the inner solar system (Bermingham et al., 2016). Ba isotope homogeneity in the early inner Solar System is evidenced by the Ba isotope compositions of H-chondrites, enstatite chondrites, eucrites, and Martian meteorites, which are all indistinguishable from terrestrial values.

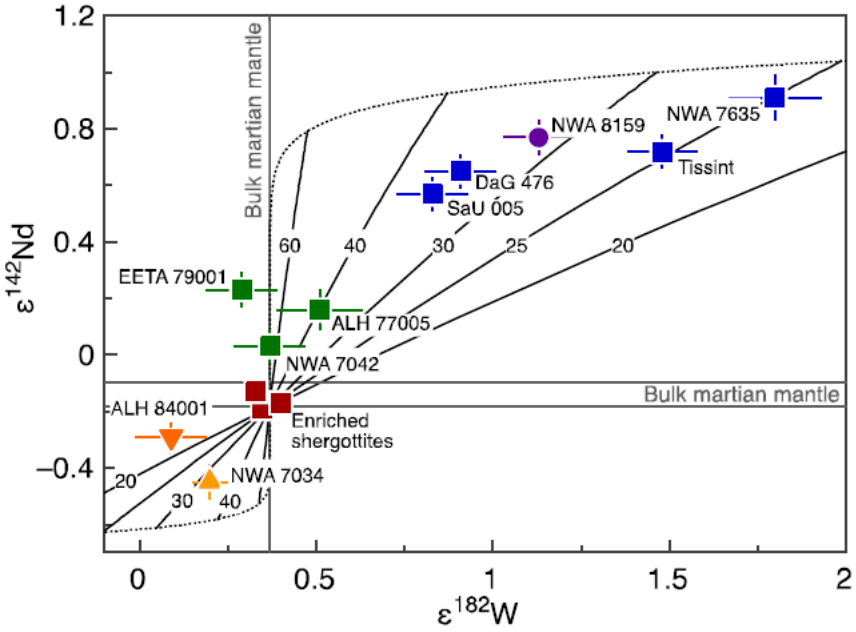


***Figure 21:*** *W–Nd isotopic diagram for Martian meteorites – NWA 4864 plots as a maroon square near the "Bulk Martian mantle" values.*

**References for NWA 2975 and pairs**


Bellucci, J. J., Whitehouse, M. J., John, T., Nemchin, A. A., Snape, J. F., Bland, P. A., & Benedix, G. K. (2017) Halogen and Cl isotopic systematics in Martian phosphates: Implications for the Cl cycle and surface halogen reservoirs on Mars. Earth and Planetary Science Letters 458, 192-202, https://doi.org/10.1016/j.epsl.2016.10.028.

Berezhnoy A.A., Bunch T.E., Ma P., Herzog G.F., Knie K., Rugel G., Faestermann T. and Korschinek G. (2008) Al-26, Be-10 and Mn-53 in Martian meteorites (abs#5306). *Meteorit. & Planet. Sci.* 45, A13.

Bermingham, K. R., Mezger, K., Scherer, E. E., Horan, M. F., Carlson, R. W., Upadhyay, D., ... & Pack, A. (2016) Barium isotope abundances in meteorites and their

implications for early Solar System evolution. *Geochimica et Cosmochimica Acta* 175, 282-298.

Borg, L. E., Brennecka, G. A., & Symes, S. J. (2016) Accretion timescale and impact history of Mars deduced from the isotopic systematics of martian meteorites. *Geochimica et Cosmochimica Acta* 175, 150-167.

Bunch, T. E., Irving, A. J., Wittke, J. H., & Kuehner, S. M. (2008) Highly evolved basaltic shergottite Northwest Africa 2800: A clone of Los Angeles. In 39th *Lunar and Planetary Science Conference,* #1953.

Cassata, W. S., & Borg, L. E. (2016) A new approach to cosmogenic corrections in 40 Ar/39 Ar chronometry: Implications for the ages of Martian meteorites. *Geochimica et Cosmochimica Acta* 187, 279-293.

Channon M.B., Boyce J.W., Stolper E.M. and Eiler J.M. (2011) Abundances of Cl, F, H and S in apatites from SNC meteorites (abs#5401). *Meteorit. & Planet. Sci.* 46, A39.

Connolly H.C. and 11 authors (2006) The Meteoritical Bulletin, No. 90. *Meteorit. & Planet. Sci.* 41, 1383-1418.

Franz H.B., Farquhar J. and Irving A.J. (2011) Acid-volatile sulfur isotopic compositions of six Shergottites (abs#2338). *42nd Lunar Plaent. Sci. Conf.* Lunar Planetary Institute @ The Woodlands.

He, Q., Xiao, L., Balta, J. B., Baziotis, I. P., Hsu, W., & Guan, Y. (2015) Petrography and geochemistry of the enriched basaltic shergottite Northwest Africa 2975. *Meteoritics & Planetary Science* 50, 2024-2044.

Humayun, M., Yang, S., Righter, K., Zanda, B., & Hewins, R. H. (2016) The Germanium Dichotomy in Martian Meteorites. In *47th Lunar and Planetary Science Conference*, # 2459.

Kruijer, T. S., Kleine, T., Borg, L. E., Brennecka, G. A., Irving, A. J., Bischoff, A., & Agee, C. B. (2017) The early differentiation of Mars inferred from Hf-W chronometry. Earth and Planetary Science Letters 474, 345-354, http://dx.doi.org/10.1016/j.epsl.2017.06.047.

Magna, T., Wiechert, U., & Halliday, A. N. (2006) New constraints on the lithium isotope compositions of the Moon and terrestrial planets. *Earth and Planetary Science Letters* 243, 336-353.

Magna, T., Hu, Y., Teng, F. Z., & Mezger, K. (2017) Magnesium isotope systematics in Martian meteorites. Earth and Planetary Science Letters 474, 419-426, http://dx.doi.org/10.1016/j.epsl.2017.07.012.

Magna, T., Day, J. M., Mezger, K., Fehr, M. A., Dohmen, R., Aoudjehane, H. C., & Agee, C. B. (2015) Lithium isotope constraints on crust–mantle interactions and surface processes on Mars. *Geochimica et Cosmochimica Acta* 162, 46-65.

McCoy, T. J., Wadhwa, M., & Keil, K. (1999) New lithologies in the Zagami meteorite: Evidence for fractional crystallization of a single magma unit on Mars. *Geochimica et Cosmochimica Acta* 63, 1249-1262.

Rumble D. and Irving A.J. (2009) Dispersion of oxygen isotopic compositions among 42 Martian meteorites determined by laser fluorination: Evidence for assimilation of (ancient) altered crust (abs#2293). *Lunar Planet. Sci.* XL, Lunar Planetary Institute @ The Woodlands.

Sanborn M.E. and Wadhwa M. (2010) Trace element geochemistry of the basaltic Shergottite Northwest Africa 2975 (abs#5294). *Meteorit. & Planet. Sci.* 45, A178.

Sharp, Z., Williams, J., Shearer, C., Agee, C., McKeegan, K. (2016) The chlorine isotope composition of Martian meteorites 2. Implications for the early solar system and the formation of Mars. Meteorit. Planet. Sci. 51, 2111-2126, doi:10.1111/maps.12591.

Shearer, C. K., Burger, P. V., Papike, J. J., McCubbin, F. M., & Bell, A. S. (2015) Crystal chemistry of merrillite from Martian meteorites: Mineralogical recorders of magmatic processes and planetary differentiation. *Meteoritics & Planetary Science* 50, 649-673.

Słaby, E., Koch-Müller, M., Förster, H. J., Wirth, R., Rhede, D., Schreiber, A., & Schade, U. (2016) Determination of volatile concentrations in fluorapatite of Martian shergottite NWA 2975 by combining synchrotron FTIR, Raman spectroscopy, EMPA, and TEM, and inferences on the volatile budget of the apatite host-magma. *Meteoritics & Planetary Science* 51, 390-406.

Słaby, E., Förster, H. J., Wirth, R., Giera, A., Birski, Ł., & Moszumańska, I. (2017) Validity of the Apatite/Merrillite Relationship in Evaluating the Water Content in the Martian Mantle: Implications from Shergottite Northwest Africa (NWA) 2975. *Geosciences* 7, 99.

Wadhwa, M., McSween Jr, H. Y., & Crozaz, G. (1994) Petrogenesis of shergottite meteorites inferred from minor and trace element microdistributions. *Geochimica et Cosmochimica Acta* 58, 4213-4229.

Ward, D., Bischoff, A., Roszjar, J., Berndt, J., & Whitehouse, M. J. (2017) Trace element inventory of meteoritic Ca-phosphates. *American Mineralogist: Journal of Earth and Planetary Materials* 102, 1856-1880.

Weisberg M.K. et al. (2008a) Met. Bull. #94. *Meteorit. & Planet. Sci.* 43, 1551-1588.

Weisberg M.K. et al. (2009b) Met. Bull #96. *Meteorit. & Planet. Sci.* 44, 1355-1397.

Weisberg M.K. et al. (2010a) Met. Bull #97. *Meteorit. & Planet. Sci.* 45, 449-493.

Weisberg M.K. et al. (2010b) Met. Bull #98. *Meteorit. & Planet. Sci.* 45, 1530-1551.

Williams, J. T., Shearer, C. K., Sharp, Z. D., Burger, P. V., McCubbin, F. M., Santos, A. R., Agee, C. B., McKeegan, K. D. (2016) The chlorine isotopic composition of Martian meteorites 1: Chlorine isotope composition of Martian mantle and crustal reservoirs and their interactions. *Meteorit. Planet. Sci.* 51, 2092-2110, doi:10.1111/maps.12647.

Wittke J.H., Bunch T.E., Irving A.J., Farmer M. and Strope J. (2006) Northwest Africa 2975: An evolved basaltic Shergottite with vesicular glass pockets and trapped melt inclusions (abs#1368). *Lunar Planet. Sci.* XXXVII Lunar Planetary Institute, Houston.

Wittke J.H., Bunch T.E., Herd C.D.K., Lapan T.J., Rumble D. Irving A.J. and Pitt D. (2010) Petrology and composition of "enriched" mafic Shergottite Northwest Africa 5718: Contrasts with Northwest Africa 2975/2986 (abs#5313). *Meteorit. & Planet. Sci*. 45, A217.

Yang, S., Humayun, M., Righter, K., Jefferson, G., Fields, D., & Irving, A. J. (2015) Siderophile and chalcophile element abundances in shergottites: Implications for Martian core formation. *Meteoritics & Planetary Science* 50, 691-714.

Yang, S., Humayun, M., Righter, K., & Peslier, H. (2018) The Contrast in Outgassing of Germanium Between Shergottites and Nakhlites. In 49th *Lunar and Planetary Science Conference*, #1681.

*K. Righter, October 2018*